



Redox conditions in the atmosphere and shallow-marine environments during the first Huronian deglaciation: Insights from Os isotopes and redox-sensitive elements



Kosuke T. Goto^{a,b,*}, Yasuhito Sekine^c, Katsuhiko Suzuki^{d,e,f}, Eiichi Tajika^c, Ryoko Senda^d, Tatsuo Nozaki^{d,f}, Ryuji Tada^a, Kazuhisa Goto^g, Shinji Yamamoto^a, Teruyuki Maruoka^h, Naohiko Ohkouchi^{f,i}, Nanako O. Ogawa^{f,i}

^a Dept. of Earth & Planetary Sci., Univ. of Tokyo, Bunkyo, Tokyo 113-0033, Japan

^b Geological Survey of Japan, AIST, Central 7, Higashi 1-1-1, Tsukuba, Ibaraki 305-8567, Japan

^c Dept. of Complexity Sci. & Engr., Univ. of Tokyo, Kashiwa, Chiba 277-8561, Japan

^d Institute for Research on Earth Evolution, JAMSTEC, Yokosuka, Kanagawa 237-0061, Japan

^e Precambrian Ecosystem Laboratory, JAMSTEC, Yokosuka, Kanagawa 237-0061, Japan

^f Submarine Resources Research Project, JAMSTEC, Yokosuka, Kanagawa 237-0061, Japan

^g International Research Institute of Disaster Science, Tohoku Univ., Sendai, Miyagi 980-8579, Japan

^h Graduate School of Life & Environ. Sci., University of Tsukuba, Tsukuba, Ibaraki 305-8572, Japan

ⁱ Institute of Biogeosciences, JAMSTEC, Yokosuka, Kanagawa 237-0061, Japan

ARTICLE INFO

Article history:

Received 27 September 2012

Received in revised form 8 June 2013

Accepted 12 June 2013

Available online 1 July 2013

Editor: J. Lynch-Stieglitz

Keywords:

Great Oxidation Event

Huronian glaciation

osmium isotope

redox-sensitive element

oxidative weathering

Paleoproterozoic

ABSTRACT

The Paleoproterozoic (2.5–2.0 Ga) is one of the most important periods in Earth's history, and was characterized by a rise in atmospheric oxygen levels and repeated (at least three) severe glaciations (the Huronian glaciations). In this study, we investigate redox conditions in the atmosphere and in shallow-marine environments immediately after the first Huronian glaciation based on the isotopic composition of Os, and the abundance of redox-sensitive elements (Os, Re, and Mo) in sedimentary rocks from the Huronian Supergroup, Canada. We found no significant authigenic enrichment of Os in the sedimentary rocks deposited during the first Huronian deglaciation. The initial isotopic composition of Os in the sediments was close to that of chondrite at the time of deposition ($^{187}\text{Os}/^{188}\text{Os} = \sim 0.11$). These results suggest that atmospheric O_2 levels were insufficient to mobilize radiogenic Os through continental weathering ($p\text{O}_2 < 10^{-5}$ – 10^{-3} present atmospheric level (PAL)). In contrast, we found enrichment of Re in the sedimentary rocks, which suggests the occurrence of oxidative weathering of Re under mildly oxidizing conditions ($> 10^{-8}$ – 10^{-5} PAL). Despite the Re enrichment, low abundances of Mo imply possible non-sulfidic conditions in shallow-marine environments at the time of deposition. Together with the results of organic carbon and sulfur analyses, we suggest that atmospheric O_2 remained at relatively low levels of around 10^{-8} – 10^{-5} PAL after the first Huronian deglaciation, which contrasts with proposed dramatic increases in O_2 after the second and third Huronian deglaciations. These results imply that the second and third Huronian glaciations may have been global events, associated with climatic jumps from severe glaciations to super-greenhouse conditions and the subsequent blooming of photosynthetic cyanobacteria in the glacial aftermath.

© 2013 Elsevier B.V. All rights reserved.

1. Introduction

The presence of a large quantity of atmospheric O_2 is one of the most significant features of the Earth, although its primitive atmosphere was essentially free of O_2 . Multiple lines of ev-

idence suggest that atmospheric O_2 levels increased dramatically during the Paleoproterozoic (2.5–2.0 Ga) Great Oxidation Event (GOE) (e.g., [Canfield, 2005](#); [Farquhar et al., 2000](#); [Karhu and Holland, 1996](#)). However, the causative mechanism of the GOE is still poorly understood. The Paleoproterozoic was also characterized by repeated (at least three) severe glaciations (the Paleoproterozoic glaciations; hereafter referred to as the Huronian glaciations) ([Kopp et al., 2005](#); [Melezhik, 2006](#); [Young et al., 2001](#)). According to previous geological and geochemical data, the atmospheric O_2 level would have been low ($p\text{O}_2 < 10^{-5}$ times the present atmospheric level (PAL)) before the Huronian glaciation

* Corresponding author at: Geological Survey of Japan, AIST, Central 7, 1-1-1 Higashi, Tsukuba, Ibaraki 305-8567, Japan. Tel.: +81 2 9849 1088; fax: +81 2 9861 3589.

E-mail address: k.goto@aist.go.jp (K.T. Goto).

(> 2.45 Ga; Bekker et al., 2004; Farquhar et al., 2000), whereas it appears that the atmosphere was highly oxidizing ($\sim 10^{-3}$ – 10^{-2} PAL) after the Huronian glaciations (< 2.2 Ga; Kopp et al., 2005; Young et al., 2001). These findings imply interactions among climate change, the evolution of the atmosphere, and life on early Earth.

Given that the Huronian glaciations took place during a period of O_2 increase, previous studies have proposed possible linkages between the atmospheric and climatic transitions (e.g., Kasting, 2005; Kirschvink et al., 2000; Melezhik, 2006). Some previous studies have proposed that climatic recovery from a severe glaciation would have induced blooming of photosynthetic cyanobacteria, leading to an increase in O_2 . Based on the abundances of redox-sensitive elements, such as Mn, Re, and Os, it is suggested that atmospheric O_2 levels increased immediately after the second and the third Huronian glaciations (Kirschvink et al., 2000; Kopp et al., 2005; Sekine et al., 2011a, 2011b). Numerical simulations also support the hypothesis that atmospheric O_2 levels may have risen in response to the repeated Huronian glaciations (Claire et al., 2006). However, the redox conditions of the atmosphere and oceans immediately after the first Huronian glaciation have been poorly investigated, although variations in the carbon isotopic composition of organic matter ($\delta^{13}C_{org}$) have been reported (Bekker and Kaufman, 2007). As atmospheric O_2 levels may have begun to increase to $\sim 10^{-8}$ – 10^{-5} PAL in the late Archean (Anbar et al., 2007; Reinhard et al., 2009), more geochemical data from across the first Huronian glaciation would help to improve our understanding of the evolution of atmospheric O_2 at the Archean–Paleoproterozoic boundary.

In this study, we investigate the redox conditions of the atmosphere and oceans immediately after the first Huronian glaciation based on the abundance of redox-sensitive elements, such as Os, Re, and Mo, in sedimentary rocks. Under anoxic atmospheric conditions, these redox-sensitive elements are immobile in the hydrological cycle. Consequently, the delivery of these elements from the continents to the oceans is highly restricted (Anbar et al., 2007). In contrast, such redox-sensitive elements are oxidized and become mobile ions that are transported from continent to ocean under oxygenated atmospheric conditions (oxidative weathering). In this case, they would be reduced in water column and trapped in anoxic ocean sediments (Anbar et al., 2007). In addition, we investigated the initial $^{187}Os/^{188}Os$ values ($^{187}Os/^{188}Os_{(i)}$) in sedimentary rocks as an indicator of oxidative continental weathering (Hannah et al., 2004; Sekine et al., 2011a). This is because continental Os contains a high proportion of radiogenic ^{187}Os , derived from radioactive decay of ^{187}Re , resulting in high $^{187}Os/^{188}Os$ values (currently ~ 1.4) relative to those of the mantle-derived or extraterrestrial sources of Os (currently ~ 0.127) (Peucker-Ehrenbrink and Ravizza, 2000). Thus, high $^{187}Os/^{188}Os_{(i)}$ in sediments may serve as evidence of the oxidative weathering of continental Os. Sekine et al. (2011a) found high concentrations of Os, Re, and Mo, together with high $^{187}Os/^{188}Os_{(i)}$, in sediments deposited immediately after the second Huronian glaciation, suggesting that oxidative weathering of continental Os occurred during the period of climatic recovery.

Here, we report Os, Re, and Mo abundances, and $^{187}Os/^{188}Os_{(i)}$, preserved in sedimentary rocks from the Ramsay Lake and Pecors formations of the Huronian Supergroup, Ontario, Canada (Fig. 1). The Ramsay Lake diamictite represents the first glaciation of the Paleoproterozoic. The basal deposits of the overlying Pecors Formation accumulated immediately after the first Huronian glaciation. In addition to redox-sensitive elements, we conducted S and organic C analyses of the sedimentary rocks to investigate both biogeochemical cycles during the deglaciation, and the host materials of redox-sensitive elements in the sediments. Based on our results, as well as previous geochemical data, we discuss the redox

conditions of the atmosphere and oceans during the first Huronian deglaciation, and the evolution of atmospheric O_2 during the Huronian glaciations.

2. Geological setting

The Huronian Supergroup is a Paleoproterozoic sedimentary succession that outcrops along the north shore of Lake Huron (Fig. 1A). The Huronian Supergroup is divided into four groups by unconformities: the Elliot Lake, Hough Lake, Quirke Lake, and Cobalt groups, in ascending stratigraphic order (Fig. 1B), and the depositional conditions of the upper three groups were mainly controlled by cyclic climate change (Bennett, 2006; Young et al., 2001). Their lithofacies vary cyclically from glacial diamictites to deltaic mudstones (or carbonates) and then fluvial quartzose sandstones (Fig. 1B; Bennett, 2006; Young et al., 2001). The deposition of the oldest sedimentary formation in the Huronian Supergroup, the Matinenda Formation, is approximately coeval to the interlayered volcanic rocks, which has been dated as 2450 ± 25 – 10 Ma (U–Pb age of zircon; Krogh et al., 1984; Prasad and Roscoe, 1996). The entire Huronian Supergroup was cut by the Nipissing diabase intrusion at 2217 ± 1.6 Ma (U–Pb age of primary baddelyite; Andrews et al., 1986). However, the detailed depositional age for the formations compose the Huronian Supergroup have yet to be reported.

The lower part of the Huronian Supergroup (below the Gowganda Formation) is considered to have been deposited in a continental rift basin (Young et al., 2001). The Ramsay Lake Formation consists mainly of matrix-supported diamictite (Bennett, 2006). Minor amounts of siltstone, wacke and arenite are also present locally (Bennett, 2006). Due to the presence of dropstones associated with laminated siltstone, the Ramsay Lake Formation has been interpreted as glaciogenic, and is recognized as the oldest glacial sediment of the Huronian Supergroup (Bennett, 2006; Robertson, 1976). The Ramsay Lake Formation is conformably overlain by the Pecors Formation, which consists mainly of mudstone, siltstone, and sandstone. Units containing flaser and wavy lenticular bedding, as well as partial Bouma sequences, have been described in the Pecors Formation, suggesting that it formed as a result of deposition by turbidity currents in the strand and offshore areas of a braid delta (Bennett, 2006; Fralick and Miall, 1989).

Several proxies have been used to reconstruct atmospheric O_2 levels from the Huronian Supergroup (Fig. 1B). The mass-independent fractionation of sulfur (MIF-S) and restricted $\delta^{34}S$ values ($\sim 0\%$) in the McKim and Pecors formations (Papineau et al., 2007) are indicative of quite low atmospheric O_2 levels at the time of deposition ($< 10^{-5}$ PAL; Pavlov and Kasting, 2002). This view of a reducing atmosphere during the deposition of the lower parts of the Huronian Supergroup (prior to the first glaciation) is supported by the presence of detrital uraninite and pyrite in the Matinenda Formation (Young et al., 2001). However, the presence of biomarkers from cyanobacteria in oil-bearing fluid inclusions within the Matinenda Formation (Dutkiewicz et al., 2006), and light $\delta^{13}C_{org}$ possibly associated with aerobic methanotrophs in the Pecors Formation (Bekker and Kaufman, 2007), may imply the presence of cyanobacteria, and the biotic production of O_2 , at the time of deposition.

In contrast, atmospheric O_2 levels may have been high when the upper Huronian Supergroup was deposited (Fig. 1B). The presence of red beds in the Lorrain Formation (Young et al., 2001), and Mn enrichment in the Gowganda Formation (Sekine et al., 2011b), suggest a highly oxidizing atmosphere ($> \sim 10^{-3}$ – 10^{-2} PAL; Rye and Holland, 1998) after the third Huronian glaciation. The absence of MIF-S (Papineau et al., 2007) and the enrichment of Os with high $^{187}Os/^{188}Os_{(i)}$ (Sekine et al., 2011a) in the Espanola Formation suggest that atmospheric O_2 levels had reached $\sim 10^{-5}$ – 10^{-3} PAL

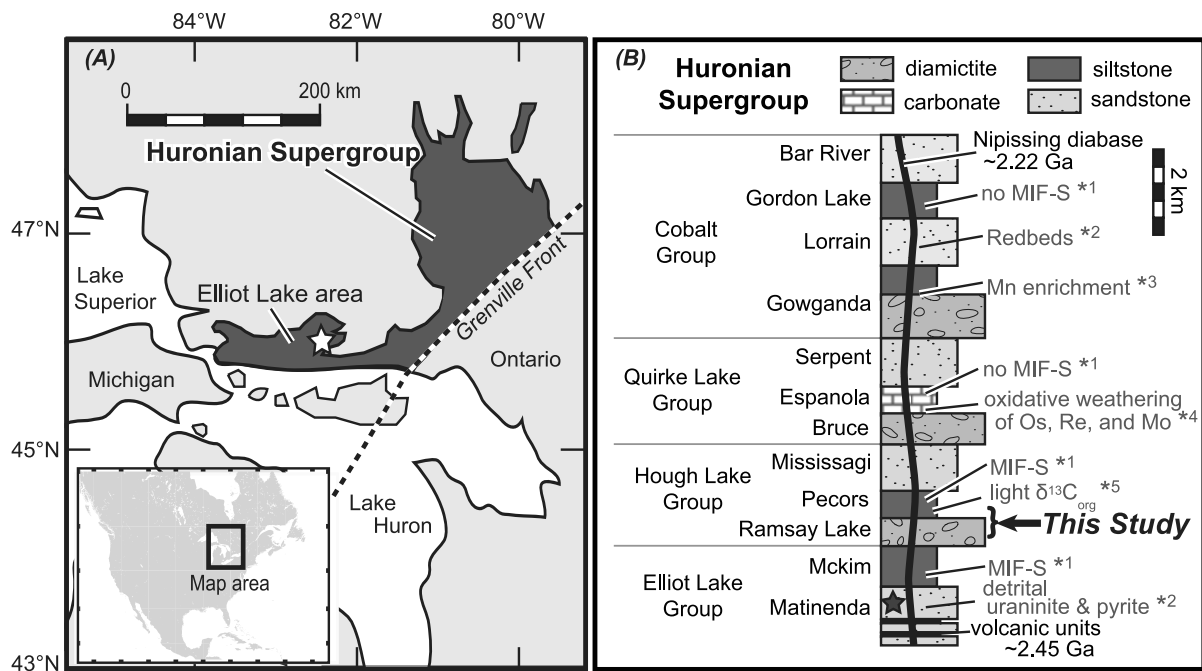


Fig. 1. Simplified geological map and stratigraphy of the Huronian Supergroup. (A) Distribution of the Huronian Supergroup. White star indicates the location of the drill core (SM0014). (B) Stratigraphy of the Huronian Supergroup and geochemical data reported previously (1: Papineau et al., 2007, 2: Young et al., 2001, 3: Sekine et al., 2011b, 4: Sekine et al., 2011a, 5: Bekker and Kaufman, 2007). Black star indicates the stratigraphic position of the cyanobacteria biomarker reported by Dutkiewicz et al. (2006).

(Rye and Holland, 1998; Sekine et al., 2011a) in the interglacial period between the second and third Huronian glaciations.

3. Sampling and lithology

Drill core samples (SM0014; Ontario Geological Survey) were collected from a site about 8 km to the north of Elliot Lake city (46°46'N, 82°60'W; Fig. 1A). The drill core covers the period from the Matinenda Formation to the lower section of the Gowganda Formation in the Huronian Supergroup (total core length of 1524 m) and contains the boundary between the Ramsay Lake and Pecors formations. This boundary consists of the matrix-supported glacial diamictite from the underlying Ramsay Lake Formation (~1 m thick) and the dark gray siltstone from the overlying Pecors Formation (~2 m thick) (Fig. 2). Here, we define the boundary between the Ramsay Lake and Pecors formations as the uppermost occurrence of dropstones.

The matrix of the Ramsay Lake Formation grades upward from a gray massive sandstone (Fig. 2D) to a dark gray clay with light gray parallel laminations (Fig. 2C), which continuously changes to a dark gray laminated siltstone in the basal section of the Pecors Formation (Fig. 2). Centimeter scale, granitic rounded dropstones were observed towards the top of the diamictite (Fig. 2C). Authigenic sulfides were also present, typically along with laminae, in the diamictite with a laminated clay-rich matrix. The Pecors Formation consists of a dark gray siltstone with parallel laminations (Fig. 2A, B). At 0.9 m above the boundary, quartz veins with a width of ~1–2 cm occurred (Fig. 2B), which could be associated with the Nipissing diabase intrusion into the Huronian Supergroup at ~2.22 Ga. Authigenic sulfides were often found in the siltstone along with laminae in the Pecors Formation (Fig. 2A). We interpret the sedimentary sequence as having been deposited during the marine transgression following deglaciation.

The bulk mineralogical and chemical compositions of the samples were determined using an X-ray Diffractometer (XRD) (X'PERT-PRO, PANalytical) and standard X-ray fluorescence technologies (XRF) (AXIOS, PANalytical), respectively, at the University of Tokyo. Based on the XRD analysis, both the matrix of the di-

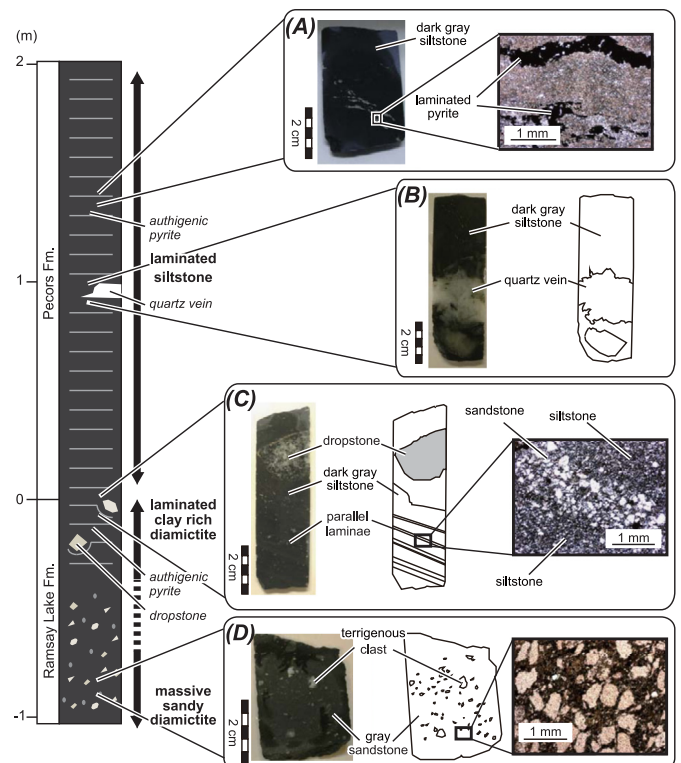


Fig. 2. Stratigraphic column from the Ramsay Lake and Pecors formations, showing details from the core samples. (A) Photograph and photomicrograph (plane-polarized light) of laminated siltstone containing laminated pyrite. (B) Core sample from ~0.9 m above the boundary between the Ramsay Lake and Pecors formations, showing a quartz vein. (C) Photograph and photomicrograph (plane-polarized light) of diamictite supported by laminated siltstone. A rounded granitic dropstone (~1 cm) is also evident. (D) Photograph and photomicrograph (plane-polarized light) of diamictite supported by a massive sandy matrix.

amictite of the Ramsay Lake Formation and the laminated siltstone of the Pecors Formation are mainly composed of quartz and mica (biotite and muscovite). The siltstone of the Pecors Formation tends to contain less quartz and more muscovite than the matrix of the underlying diamictite. The results of XRF analyses are summarized in Sekine et al. (2011b).

4. Analytical methods

4.1. Sample preparation

We measured whole rock concentrations and the isotopic compositions of Os and Re, the concentrations of Mo and U, total sulfur (TS) and total organic carbon (TOC) contents, and $\delta^{13}\text{C}_{\text{org}}$. The surface layer of each drill core sample was removed using a diamond cutter, before it was cleaned in an ultrasonic bath with distilled water. For Os, Re, Mo, and U analyses, the surface of the cut samples was polished carefully with corundum powder to remove contamination from the diamond cutter before ultrasonication. For the diamictite samples, we analyzed the matrix. The cleaned samples were pulverized in an agate mortar.

4.2. Re–Os analysis

Powdered samples of 0.4–1.0 g were used for the Re–Os analyses. We analyzed granitic cobbles from the diamictite and quartz veins within the siltstone in addition to the bulk rock geochemical analysis. The analytical procedure was based on isotope dilution combined with Carius tube digestion (Shirey and Walker, 1995), carbon tetrachloride and solvent extractions (Cohen and Waters, 1996), microdistillation (Birck et al., 1997), and column separations by anion exchange chromatography (Morgan et al., 1991). Powdered samples were loaded into Carius tubes with known amounts of ^{190}Os and ^{185}Re spike solutions, and then the dissolution media (5 ml) were added. In this study, two types of dissolution media were used for the Re–Os analysis: $\text{CrO}_3\text{--H}_2\text{SO}_4$ digestion and inverse *aqua regia* ($\text{HCl}:\text{HNO}_3 = 1:3$) digestion. Prior to the $\text{CrO}_3\text{--H}_2\text{SO}_4$ digestion, the $\text{CrO}_3\text{--H}_2\text{SO}_4$ acid was purified using CHCl_3 extraction and N_2 -sparging (Selby and Creaser, 2003). The $\text{CrO}_3\text{--H}_2\text{SO}_4$ dissolution medium has been proposed to dissociate detrital components much less efficiently than inverse *aqua regia*, and has been used in recent Re–Os analysis of organic-rich sediments to minimize the effects of non-hydrogenous Os and Re (Kendall et al., 2004; Selby and Creaser, 2003). The Carius tubes were sealed and heated for 48 h at 240 °C for $\text{CrO}_3\text{--H}_2\text{SO}_4$ (Selby and Creaser, 2003), and 24 h at 220 °C for inverse *aqua regia* (Kato et al., 2005) to equilibrate the samples and spike solutions. After heating, Os and Re were separated by CCl_4 solvent extraction. Subsequently, Os was back-extracted from CCl_4 into HBr and purified using the microdistillation method. Rhenium was separated from the aqueous phase by column separation using Muromac's AG 1-X8 anion exchange resin.

The isotopic compositions of Os and Re were measured using negative thermal ionization mass spectrometry (NTI–MS; ThermoFinnigan TRITON) at JAMSTEC (Kato et al., 2005). To reduce blank levels and organic interferences during the Os and Re measurements, Os and Re were loaded on a high purity Pt filament that had been baked in air to high temperatures for three minutes prior to loading. The samples were covered with 10,000 ppm $\text{Ba}(\text{NO}_3)_2$ solution (10 μl). The instrumental mass fractionation of Os was corrected by normalizing the measured $^{192}\text{Os}/^{188}\text{Os}$ to 3.08271 (Nier, 1937). Rhenium isotopic ratios were measured by the total evaporation method (Suzuki et al., 2004). All data were corrected for procedural blank levels of 9–12 pg for Re and 0.8–2.2 pg for Os, $^{187}\text{Os}/^{188}\text{Os} = 0.268\text{--}0.296$ for Os ($n = 3$, $\text{CrO}_3\text{--H}_2\text{SO}_4$ digestion). The magnitude of the procedural blanks

relative to the amount of Re and Os from the samples was less than 1% for Re and 3% for Os. In-house standard samples were measured repeatedly, and excellent reproducibility was achieved (Kato et al., 2005); the $^{187}\text{Os}/^{188}\text{Os}$ ratios and Re and Os concentrations of the reference material (JA-2; Geological survey of Japan (GSJ)) samples are 0.2092 ± 0.0078 (2σ) and 46.7 ± 1.6 and 11.4 ± 1.5 ppt, respectively ($n = 5$). The results of Re–Os analyses are summarized in Supplementary Table 1.

4.3. Mo and U analysis

For Mo and U analysis, powdered samples (~100 mg) were completely dissolved in an $\text{HNO}_3\text{--HClO}_4\text{--HF}$ dissolution medium (Kato et al., 2005). This is because Si can be precipitated at the inlet system of the ICP–MS during the measurements. Accordingly, Si needs to be removed from the solution as SiF_4 during the digestion. Samples were finally dissolved in 2% HNO_3 . Trace HF was also added to each solution to ensure Mo remained stable in solution. Concentrations of Mo and U in the solutions were measured with ICP–MS (7500ce; Agilent) at JAMSTEC. We also measured Mo and U concentrations in JA-2. The difference between our laboratory data and the recommended values for JA-2 (Imai et al., 1995) was mostly <5%.

4.4. Sulfur analysis

The TS content of the powdered samples was determined using EA/IRMS (Elemental Analyzer/Isotope-Ratio Mass Spectrometer) system (Isoprime-EA, Isoprime Ltd.) at University of Tsukuba (Maruoka et al., 2005). Powdered samples (2–5 mg) were loaded into tin cups with V_2O_5 powder (~3 mg) as oxidant before being introduced into the EA/IRMS system. The TS content of the samples was determined by calibrated ion currents with a mass-to-charge (m/z) ratio of 64 in the isotope-ratio mass spectrometer. The reagent grade of Ag_2S (Wako Pure Chemical Industries, Ltd.) and the reference material (JSD-3; GSJ) were used in the calibration of the sulfur content. Measurements were performed four times for each sample, and the concentrations were determined from the average of these four measurements. Analytical uncertainties were expressed as one standard deviation of the repeated measurements.

4.5. Organic carbon analysis

$\delta^{13}\text{C}_{\text{org}}$ and TOC measurements were carried out using modified online version of the Finnigan Delta Plus XP isotope-ratio mass spectrometer coupled to Flash EA1112 elemental analyzer (EA/IRMS) through ConFlo III interface at JAMSTEC (Ohkouchi et al., 2005; Sekine et al., 2010). The EA/IRMS system was modified to improve sensitivity (Ogawa et al., 2010). Powdered samples (~300 mg) were treated with 4N HCl to remove carbonate. The samples were washed several times with distilled water and dried overnight. The dried samples (~30 mg) were loaded into tin cups and then introduced into the EA/IRMS system. Total organic carbon content in the samples was determined by calibrated ion currents with m/z ratios of 44, 45, and 46 in the isotope-ratio mass spectrometer. $\delta^{13}\text{C}_{\text{org}}$ were expressed using the conventional δ notation against the VPDB standard: $\delta^{13}\text{C} = (^{13}\text{R}_{\text{sample}}/^{13}\text{R}_{\text{standard}} - 1) \times 1000$, where ^{13}R is $^{13}\text{C}/^{12}\text{C}$ ratio. The U and Mo concentrations, TS and TOC content, and $\delta^{13}\text{C}_{\text{org}}$ are summarized in Supplementary Table 2.

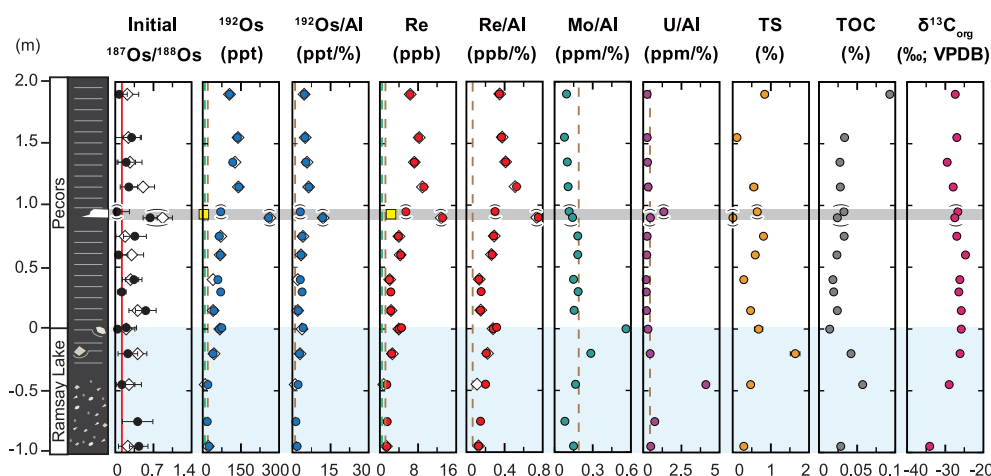


Fig. 3. Stratigraphy and associated geochemical profiles from the boundary between the Ramsay Lake and Pecors formations showing $^{187}\text{Os}/^{188}\text{Os}_{(i)}$, abundances of ^{192}Os , Re, Mo, and U, TS and TOC, and $\delta^{13}\text{C}_{\text{org}}$ in the sedimentary rocks. Sample proximity to the quartz vein is shown in parentheses. The Re–Os results based on $\text{CrO}_3\text{--H}_2\text{SO}_4$ digestion are represented by filled circles, and the results from the inverse *aqua regia* digestion are represented by open diamonds. Initial $^{187}\text{Os}/^{188}\text{Os}$ values were calculated using the ^{187}Re decay constant $\lambda = 1.666 \times 10^{-11} \text{ yr}^{-1}$ (Smoliar et al., 1996) and a probable depositional age of $2.4 \pm 0.05 \text{ Ga}$ (Young et al., 2001). The errors associated with the $^{187}\text{Os}/^{188}\text{Os}_{(i)}$ were derived from analytical errors and uncertainty in the depositional age. The brown dashed lines in the plots of ^{192}Os and Re concentrations, and $^{192}\text{Os}/\text{Al}$, Re/Al, Mo/Al, and U/Al ratios, show the average values in the upper continental crust (Anbar et al., 2007; Peucker-Ehrenbrink and Jahn, 2001). The green dashed lines and yellow squares in the plots of Re and Os concentrations show the same values for dropstones found in the diamictite unit and those of the quartz veins in the siltstone unit respectively. The red solid line in the initial $^{187}\text{Os}/^{188}\text{Os}$ plot shows the value of the mantle-derived Os at the time of deposition ($^{187}\text{Os}/^{188}\text{Os} = 0.11$; Shirey and Walker, 1998). The glacial diamictite unit is shaded light blue, and the position of the quartz vein is shaded gray. (For interpretation of the references to color in this figure legend, the reader is referred to the web version of this article.)

5. Results and discussion

5.1. Geochemical records of Re and Os

5.1.1. Osmium and Re concentrations

Fig. 3 shows variations in the concentrations of ^{192}Os (non-radiogenic Os) and Re across the boundary between the Ramsay Lake and Pecors formations. We also measured the concentration of ^{192}Os and Re in granitic cobbles collected from the diamictite of the Ramsey Lake Formation. As these granitic cobbles were carried from the continent by icebergs (dropstones), these values could represent the typical ^{192}Os and Re concentrations of one of the major sources of detrital material. Fig. 3 indicates that most of the sedimentary rock samples (matrix component) have concentrations of ^{192}Os and Re significantly higher than those of the granitic cobbles ($\text{Os} = \sim 3 \text{ ppt}$; $\text{Re} = \sim 20 \text{ ppt}$) and average upper continental crust ($^{192}\text{Os} = \sim 13 \text{ ppt}$ and $\text{Re} < 400 \text{ ppt}$; Peucker-Ehrenbrink and Jahn, 2001). To examine the degree of authigenic enrichment, we have normalized them with the Al content of each sample (Tribouillard et al., 2006). The enrichment of ^{192}Os is not observed when normalized by Al content. However, Re/Al values in the Pecors Formation are up to several times higher than the levels in average upper continental crust (Fig. 3), which is indicative of the authigenic enrichment of Re in the sediments deposited in the glacial aftermath. Fig. 3 also shows that there are no significant differences between the samples treated with $\text{CrO}_3\text{--H}_2\text{SO}_4$ acid (filled circles) and those treated with inverse *aqua regia* (open diamonds) dissolution medium. Given that $\text{CrO}_3\text{--H}_2\text{SO}_4$ acid dissociates detrital components less efficiently than inverse *aqua regia* (Selby and Creaser, 2003), this measured similarity in the results from different dissolution media suggests that the contribution of ^{192}Os and Re from the detrital components was very small. These results support the conclusion that authigenic Os and Re are predominant in ^{192}Os and Re in these sediments, although $^{192}\text{Os}/\text{Al}$ and Re/Al values suggest that a remarkable enrichment occurs only for Re in the sediments.

Previous studies show that several metamorphic events associated with the Penokean Orogeny (around 1.9–1.7 Ga) affected the Huronian Supergroup (Fedo et al., 1997; McLennan et al., 2000;

Ono and Fayek, 2011), which could have overprinted and/or disturbed the Re–Os system. The Re–Os isochron plot of the results of the $\text{CrO}_3\text{--H}_2\text{SO}_4$ digestion is shown in Fig. 4. This figure shows that the Re–Os data, excluding two samples near the quartz vein, yields an Re–Os date of $2396 \pm 160 \text{ Ma}$, with an $^{187}\text{Os}/^{188}\text{Os}_{(i)}$ of 0.25 ± 0.42 (Fig. 4). The obtained Re–Os isochron age is consistent with a possible depositional age of the Ramsay Lake and Pecors formations ($\sim 2.4 \text{ Ga}$) judging from the age constraints for the Huronian Supergroup, suggesting no large-scale disturbance in the Re–Os system due to more recent metamorphic events at $\sim 1.9\text{--}1.7 \text{ Ga}$. Fig. 4 also shows that all of the measured data fall inside the range expected to develop over a period of 2.4 Ga given $^{187}\text{Os}/^{188}\text{Os}_{(i)}$ that are intermediate between the non-radiogenic mantle-derived value at the time of deposition (~ 0.11 ; Shirey and Walker, 1998) and a possible radiogenic continental value (~ 1.0 ; Sekine et al., 2011a). As post-depositional perturbations in the Re–Os system should have resulted in a very large degree of scatter in the Re–Os isochron plot (Kendall et al., 2009; Rooney et al., 2011), these results suggest that the Re–Os system suffered relatively little disturbance or overprinting by later metamorphic and alteration events.

Although large-scale post-depositional additions/losses of Os and Re appear not to have occurred in our samples, a small-scale perturbation of the Re–Os system might have been caused by the intrusion of the quartz veins. In the quartz veins, the concentrations of ^{192}Os and Re ($^{192}\text{Os} = 7 \text{ ppt}$ and $\text{Re} = 2.8 \text{ ppb}$) were lower than those in the sedimentary rock samples. However, the sample close to the quartz veins (at 0.9 m above the boundary) has high concentrations of ^{192}Os and Re (Fig. 3). As shown below in this section, the $^{187}\text{Os}/^{188}\text{Os}_{(i)}$ of this sample is significantly higher than the other samples (Fig. 3). Since quartz veins are unlikely to be the source of Os and Re, these results may imply that the intrusion of quartz veins resulted in the small-scale mobilization (within 10 cm; the typical size of the rock samples) of Os and Re, leading to a small degree of scatter in the isochron diagram (Fig. 4).

As Os and Re are chalcophilic elements, they could be hosted in authigenic sulfide minerals in the sediments (Hannah et al., 2004; Sekine et al., 2011a). Os and Re concentrations in pyrite crystals

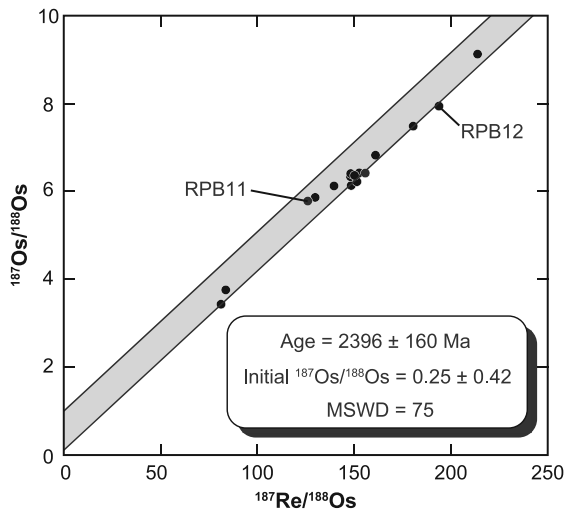


Fig. 4. Re–Os isochron diagram for samples from the boundary between the Ramsay Lake and Pecors formations using $\text{CrO}_3\text{--H}_2\text{SO}_4$ digestion as the dissolution medium. The Re–Os data that excludes the samples from near the quartz vein (RPB11 and RPB12; see Supplementary Tables 1 and 2) yielded an Re–Os date of 2396 ± 160 Ma with an $^{187}\text{Os}/^{188}\text{Os}_{(i)}$ of 0.25 ± 0.42 using *Isoplot 3.0* (Ludwig, 2003). Errors are $2\sigma_m$. The gray area represents the range expected to develop over a period of 2.4 Ga given the $^{187}\text{Os}/^{188}\text{Os}_{(i)}$ that are intermediate between the non-radiogenic mantle-derived value (~ 0.11 ; Shirey and Walker, 1998) and a possible radiogenic continental values (~ 1 ; Sekine et al., 2011a).

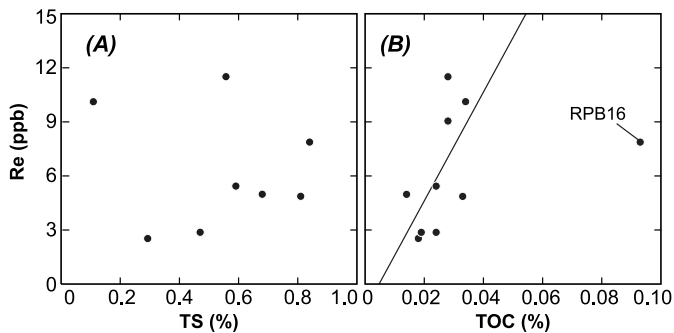


Fig. 5. Crossplots of (A) Re concentration and TS content, and (B) Re concentration and TOC content in samples from the Pecors Formation, but excluding those samples near the quartz vein (RPB11 and RPB12; see Supplementary Tables 1 and 2). The relationship between Re concentration and TOC shows a weak positive correlation, with one outlier (RPB16), and the correlation coefficient of the least squares straight line is 0.61.

separated using heavy liquids ($\text{Os} = \sim 100$ ppt and $\text{Re} = \sim 3$ ppb in the Ramsay Lake Formation; $\text{Os} = \sim 300$ ppt and $\text{Re} = \sim 10$ ppb in the Pecors Formation) are comparable to those of the bulk rock samples. If the pyrite is the main host material of Os and Re, their concentrations in the bulk samples should be much lower than those actually measured, given the low TS contents ($< 2\%$; Fig. 3). In addition, the variation in TS in the Pecors Formation does not show any clear correlation with the concentration of Os or Re (Fig. 5). Thus, it is unlikely that authigenic sulfide minerals are the major host material of Os and Re in our sedimentary rock samples. Considering that organic materials adsorb Os and Re dissolved in the water column, they are also capable of hosting Os and Re in marine sediments (e.g., Ravizza and Turekian, 1992; Yamashita et al., 2007). Fig. 3 shows that TOC also increases upwards in the Pecors Formation, as does the concentration of Os and Re. Fig. 5 shows that there is a weak correlation between the Re and TOC abundances, except for one sample (RPB16). Although the TOC content of our samples was significantly lower (< 0.04 wt%) compared with those in previous studies that reported authigenic enrichment of Os and Re (TOC > 1 wt%; e.g.,

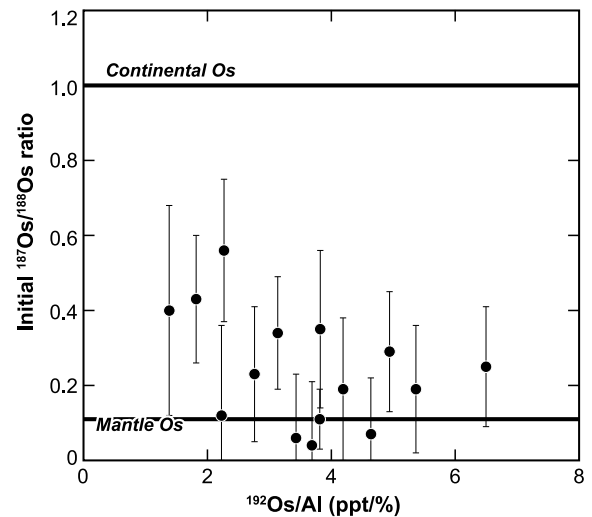


Fig. 6. Crossplot of $^{187}\text{Os}/^{188}\text{Os}_{(i)}$ and $^{192}\text{Os}/\text{Al}$ in samples, except the samples near the quartz vein (RPB11 and RPB12). The samples with lower $^{192}\text{Os}/\text{Al}$ values tend to show more radiogenic $^{187}\text{Os}/^{188}\text{Os}$, suggesting that the proportion of detrital Os may not be negligible for the samples with very low authigenic Os abundance.

Anbar et al., 2007), these results may indicate that organic materials are one of the major host materials (i.e., possibly existing as hydrogenous Os and Re) in the sediments.

5.1.2. Initial $^{187}\text{Os}/^{188}\text{Os}$ ratios

Fig. 3 shows the variation in $^{187}\text{Os}/^{188}\text{Os}_{(i)}$ obtained from the present $^{187}\text{Os}/^{188}\text{Os}$ and $^{187}\text{Re}/^{188}\text{Os}$ ratios of the sediments using a depositional age of 2.4 ± 0.05 Ga. Some of the samples with lower $^{192}\text{Os}/\text{Al}$ values tend to show more radiogenic $^{187}\text{Os}/^{188}\text{Os}$ (Fig. 6). Because detrital Os usually holds radiogenic $^{187}\text{Os}/^{188}\text{Os}$ values (Peucker-Ehrenbrink and Jahn, 2001), these results may reflect that the contribution of detrital source of Os to the $^{187}\text{Os}/^{188}\text{Os}$ values would not be negligible for the samples with very low levels of hydrogenous Os. However, most of the $^{187}\text{Os}/^{188}\text{Os}_{(i)}$ based on the $\text{CrO}_3\text{--H}_2\text{SO}_4$ dissolution medium (filled circles) are as low as the chondritic value at the time of deposition (~ 0.11 ; Shirey and Walker, 1998) within their errors (Fig. 3). The chondritic $^{187}\text{Os}/^{188}\text{Os}_{(i)}$ can be explained by the absence of oxidative weathering of continental Os and/or an increased hydrothermal Os flux to the oceans. Assuming the modern continental Os flux (~ 1550 mol/yr; Levasseur et al., 1999) with an $^{187}\text{Os}/^{188}\text{Os}$ of ~ 1.0 (Sekine et al., 2011a), however, extremely large hydrothermal Os flux ($> \sim 50$ times of the modern flux) would be required to reduce the seawater $^{187}\text{Os}/^{188}\text{Os}$. Such increased hydrothermal activity has been suggested for the Mesozoic periods (Tejada et al., 2009; Turgeon and Creaser, 2008). Nevertheless, these $^{187}\text{Os}/^{188}\text{Os}$ anomalies are often accompanied by high ^{192}Os concentrations (~ 800 ppt), which is contrast to the present study. Although we cannot rule out the potential increased hydrothermal Os inputs, the chondritic $^{187}\text{Os}/^{188}\text{Os}$ value in our samples seems likely due to the absence of oxidative weathering of Os.

Previous studies have revealed that $^{187}\text{Os}/^{188}\text{Os}_{(i)}$ in late-Archean and Paleoproterozoic shales have also been close to the chondritic values, suggesting little input of continental radiogenic Os into the oceans under low atmospheric O_2 conditions (Anbar et al., 2007; Hannah et al. 2004, 2006; Yang et al., 2009). Our results also suggest that the measured low $^{187}\text{Os}/^{188}\text{Os}_{(i)}$ in the sedimentary rock samples are evidence for low atmospheric O_2 levels during, and immediately after, the first Huronian glaciation. This conclusion contrasts with the recent findings of high $^{187}\text{Os}/^{188}\text{Os}_{(i)}$ in shallow-marine sediments deposited in the aftermath of the second Huronian glaciation (Sekine et al., 2011a).

More detailed discussion on the comparison with the first Huronian glaciation will be given below in Section 6.2.

5.2. Mo and U abundances, and $\delta^{13}\text{C}_{\text{org}}$

Fig. 3 shows the abundance of Mo and U, and $\delta^{13}\text{C}_{\text{org}}$ levels, across the boundary between the Ramsey Lake and Pecors formations. Most of the Mo/Al and U/Al values in the Pecors Formation are close to, or less than, those of the upper crust (Fig. 3). Our results of the low abundance of Mo and enrichment of Re are in contrast to the previous results that show the enrichment of Mo associated to high levels of Re found in the 2.5-Ga Mount McRae Shale in the Hamersley group (Anbar et al., 2007) and the 2.3-Ga siltstone interval deposited immediately after the Bruce glaciation in the Huronian Supergroup (Sekine et al., 2011a). However, our results are consistent with the results of previous studies that analyzed the 2.45–2.15 Ga sedimentary rocks in the Transvaal Supergroup, South Africa (Siebert et al., 2005; Wille et al., 2007). In the Ramsey Lake Formation, there are a few samples with high concentrations of U and Mo (Fig. 3). These non-systematic enrichments in the diamictite may have been caused by inclusions of detrital minerals having very high concentrations of U and Mo, such as detrital uraninite and pyrite. In fact, previous studies have reported the presence of detrital uraninite and pyrite in the Matinenda Formation of the Huronian Supergroup (Ono and Fayek, 2011; Young et al., 2001).

Our results of TS and TOC contents show no significant variations throughout the section. Because organic materials and sulfide minerals tend to be preserved in the sediments in reducing bottom water, these results may indicate no significant changes in the redox condition of the bottom seawater at the local depositional setting. The organic carbon isotopic analyses revealed that $\delta^{13}\text{C}_{\text{org}}$ values gradually increase from -34‰ to -25‰ in the Ramsey Lake diamictite, but then remain constant at around -25‰ in the Pecors siltstone (Fig. 3). Although TOC content was low throughout the section (< 0.1 wt%), the absence of any correlation between TOC content and $\delta^{13}\text{C}_{\text{org}}$ values rules out the possibility of artificial contamination during the analytical procedure (Supplementary Fig. S1). Therefore, we concluded that $\delta^{13}\text{C}_{\text{org}}$ compositions mainly reflect the variation of biomass during the deglaciation. A similar $\delta^{13}\text{C}_{\text{org}}$ variation (positive shift of $\delta^{13}\text{C}_{\text{org}}$) was observed in sedimentary rocks deposited in the aftermath of the second Huronian glaciation (Sekine et al., 2011a). During the glaciations, primary productivity would have been limited in the oceans. As $\delta^{13}\text{C}_{\text{org}}$ values of -25‰ are typical over Earth history (Schidlowski, 2001), the positive shift of $\delta^{13}\text{C}_{\text{org}}$ suggests that primary productivity by photosynthesis had become dominant in the aftermath of the first Huronian glaciation. Alternatively, the activity of methanotrophs may have varied significantly, while primary productivity by photosynthesis has remained constant during this period.

Bekker and Kaufman (2007) have also investigated variations in $\delta^{13}\text{C}_{\text{org}}$ values in sedimentary rocks of the McKim and Pecors formations, including at the boundary between the Ramsey Lake and Pecors formations. In contrast to our results, they found a negative $\delta^{13}\text{C}_{\text{org}}$ shift from -25‰ to -35‰ in shallow-marine sediments across the boundary, and interpret the measured negative $\delta^{13}\text{C}_{\text{org}}$ values in the Pecors Formation as evidence of high levels of biological CH_4 production and enhanced oxidative CH_4 recycling by methanotrophs around the redox boundary. Given the findings of Bekker and Kaufman (2007), the $\delta^{13}\text{C}_{\text{org}}$ variation measured here implies that both biological CH_4 and O_2 productions occurred, possibly predominantly in the aftermath of the first Huronian glaciation. However, relative proportion of biological CH_4 and O_2 productions may have differed depending on location in the oceans at the time of deposition, possibly resulting in considerable variations in the depth of the redox boundary in the oceans: i.e., biological CH_4

would have been dominant below the redox boundary and biological O_2 production would have been dominant above it (Bekker and Kaufman, 2007).

6. Implications for evolution of atmospheric O_2 during the Huronian glaciations

6.1. Redox conditions during the first Huronian deglaciation

Given the presence of MIF-S in the McKim and Pecors formations, and detrital uraninite and pyrite in the Matinenda Formation (Papineau et al., 2007; Young et al., 2001, Fig. 1B), atmospheric O_2 levels were likely to have been low ($< 10^{-5}$ PAL) at the time of deposition of the lower parts of the Huronian Supergroup (below the Pecors Formation). The high-resolution Os isotope analysis reported here from the boundary between the Ramsey Lake and Pecors formations (Fig. 3) suggests that atmospheric O_2 levels would have remained low ($< 10^{-5}$ – 10^{-3} PAL; Rye and Holland, 1998; Sekine et al., 2011a) even during the period of climate recovery following the first Huronian glaciation.

Although atmospheric O_2 levels did not reach $\sim 10^{-5}$ – 10^{-3} PAL in the aftermath of the first Huronian glaciation, the variations found in Re and Mo concentrations in these sediments, combined with previously reported sulfur isotopic composition (Papineau et al., 2007), suggest that the atmosphere would have been mildly oxidizing ($\sim 10^{-8}$ – 10^{-5} PAL; Reinhard et al., 2009) at the time of deposition. Because the redox potentials of Re and Mo (-0.15 to 0 V at pH 6 to 7; Brookins, 1988) are lower than those of Os ($+0.1$ to $+0.35$ V at pH 6 to 7; Brookins, 1988), oxidative weathering of continental Re and Mo would occur even under mildly oxidizing atmospheric conditions (Reinhard et al., 2009). In fact, recent geochemical studies suggest that oxidative weathering of Re and Mo might have occurred in the late Archean at around 2.6–2.5 Ga under mildly oxidizing conditions (Anbar et al., 2007; Kendall et al., 2010; Siebert et al., 2005; Wille et al., 2007). Our finding of authigenic enrichment of Re in the Pecors Formation suggests that oxidative weathering of Re occurred, possibly due to a small increase in biologic O_2 production and/or active hydrological cycles, during climatic recovery from the glaciation (Fig. 3).

The absence of Mo enrichment in the Pecors Formation (Fig. 3) is likely due to the different mechanisms associated with the removal of Re and Mo from seawater into sediments. Both Re and Mo are removed from seawater into reducing sediments (Crusius et al., 1996; Yamashita et al., 2007). Nevertheless, authigenic accumulation of Mo proceeds under sulfidic conditions by the reaction of MoO_4^{2-} with H_2S , forming $\text{MoO}_{4-x}\text{S}_x^{2-}$ (Crusius et al., 1996; Russell and Morford, 2001). Accordingly, the accumulation of Mo is controlled by sulfide availability in seawater; whereas the accumulation of Re is not limited by sulfide concentrations (Crusius et al., 1996; Yamashita et al., 2007). Thus, our Re and Mo records suggest that shallow-marine environments would not have been highly sulfidic at the local depositional setting during the first Huronian deglaciation. Such a view of non-sulfidic shallow ocean conditions is consistent with the results from sedimentary rocks in the Transvaal Supergroup (Siebert et al., 2005; Wille et al., 2007). Additionally, the sulfur isotopic compositions prior to 2.3 Ga in both the Huronian and Transvaal supergroups suggest low levels of sulfate reducing bacterial activity at the time of deposition (Guo et al., 2009; Papineau et al., 2007). These results possibly support the idea of widespread non-sulfidic conditions in the oceans in Paleoproterozoic before the first Huronian glaciation, although further investigations at different supergroups are required to conclude.

6.2. O_2 evolution in response to the repeated glaciations

It has been proposed that the Paleoproterozoic glaciations would have promoted the oxygenation of Earth's surface envi-

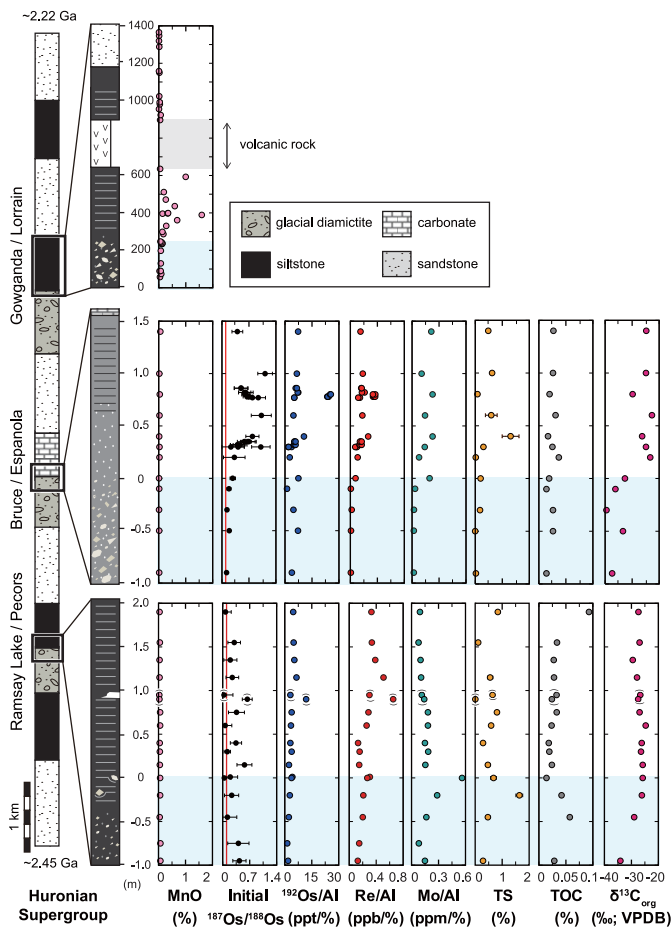


Fig. 7. Comparison of the profiles of various redox proxies in the sedimentary rocks deposited immediately after the Huronian glaciations: Mn abundance, $^{187}\text{Os}/^{188}\text{Os}_{(i)}$, $^{192}\text{Os}/\text{Al}$, Re/Al , and Mo/Al ratios, TS and TOC contents, and $\delta^{13}\text{C}_{\text{org}}$ values. Geochemical data for the second and the third Huronian glaciations are based on Sekine et al. (2011a, 2011b).

ronment in the GOE (e.g., Kirschvink et al., 2000; Kopp et al., 2005). Recent geochemical studies have provided evidence of a synchronicity between climatic recovery from the glaciations and oxygenation during the second and third Huronian glaciations, suggesting that greenhouse conditions in the aftermath of these severe glaciations would have supplied large amounts of nutrients to photosynthetic bacteria, leading to a rise in atmospheric O_2 levels (Kirschvink et al., 2000; Sekine et al., 2011a, 2011b). Nevertheless, our results suggest that atmospheric O_2 would not have increased dramatically in the aftermath of the first Huronian glaciation.

Fig. 7 summarizes a comparison of the results of the enrichment and/or depletion of redox sensitive elements in sediments deposited immediately after the three glaciations recorded in the Huronian Supergroup. Based on these geochemical data combined with previous study, we compared the atmospheric O_2 level of the Huronian glaciations, although the estimated $p\text{O}_2$ values may have an uncertainty of one order of magnitude (Fig. 8). Oxidative weathering of Re would have occurred in the aftermath of both the first and the second Huronian glaciations. However, obvious Os enrichment, with high $^{187}\text{Os}/^{188}\text{Os}_{(i)}$, occurred only after the second Huronian glaciation (Fig. 7). These results suggest that atmospheric O_2 increased to $\sim 10^{-5}$ – 10^{-3} PAL after the second Huronian glaciation, whereas it remained below $\sim 10^{-5}$ – 10^{-3} PAL during, and in the aftermath, of the first Huronian glaciation. As the redox potential of Mn is the highest (+0.5 V at pH 6–7; Brookins, 1988) among redox sensitive elements, Mn enrichments in the sediments

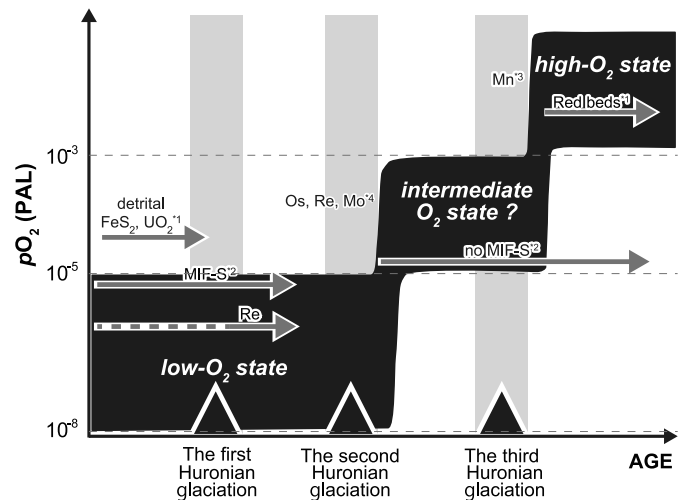


Fig. 8. Schematic diagram of the possible evolution of atmospheric O_2 levels (black solid line) during the Huronian glaciations based on geochemical evidence from the Huronian Supergroup obtained in the present and previous studies (1: Young et al., 2001, 2: Papineau et al., 2007, 3: Sekine et al., 2011b, 4: Sekine et al., 2011a). Atmospheric O_2 would have been around $\sim 10^{-8}$ – 10^{-5} PAL (Anbar et al., 2007; Pavlov and Kasting, 2002; Reinhard et al., 2009) in the aftermath of the first Huronian glaciation. However, it would have increased to $\sim 10^{-5}$ – 10^{-3} PAL (Rye and Holland, 1998; Sekine et al., 2011a) and $\sim 10^{-3}$ – 10^{-2} PAL (Rye and Holland, 1998) in the aftermath of the second and third Huronian glaciations, respectively. Note that the atmospheric O_2 levels shown in this figure are derived from the previous estimations based on thermodynamic equilibrium calculations of mineral assemblages in paleosols and sediments, comparisons of oxidative potentials of redox sensitive elements, and criteria for the appearance of MIF-S obtained from a photochemical model. These O_2 levels are approximate values, which may have an associated error of one order of magnitude.

can constrain an accumulation of high levels of atmospheric O_2 ($> 10^{-3}$ – 10^{-2} PAL; Rye and Holland, 1998). Enrichment of Mn has only been found in sediments deposited after the third Huronian glaciation (Fig. 7), suggesting that an accumulation of atmospheric $\text{O}_2 > 10^{-3}$ – 10^{-2} PAL would not have occurred until the termination of the third Huronian glaciation (Sekine et al., 2011b).

Despite uncertainties due to the lack of continuous geochemical records, the comparison of results derived from the various proxies allows us to develop a possible scenario for O_2 evolution in response to the glacial cycles in the Paleoproterozoic (Fig. 8). We propose that atmospheric O_2 levels would have jumped from a lower O_2 to a higher O_2 state in the aftermath of the glaciations in the Paleoproterozoic (Goldblatt et al., 2006). As for the first Huronian glaciation, the atmospheric O_2 levels seem to have remained around 10^{-8} – 10^{-5} PAL (low- O_2 states; Fig. 8). There are two possible explanations of why O_2 levels did not increase markedly in the first Huronian deglaciation. If the first Huronian glaciation was not a global-scale glaciation, which would have been associated with a climatic jump to a hot and humid condition in the glacial aftermath (Kirschvink et al., 2000; Hoffman and Schrag, 2002), the increase in surface temperature after the glaciation would not have been high sufficient to lead to high levels of net primary productivity. In fact, the presences of a cap carbonate unit (Espanola Formation; Fig. 1B) following the second Huronian glaciation (Bekker et al., 2005), and an intensely weathered quartzose sandstone unit (Lorrain Formation; Fig. 1B) overlying the youngest Huronian diamictite (Sekine et al., 2010), suggest sudden climatic shifts from icehouse to super-greenhouse conditions after these two glacial events. However, there is no clear geological evidence for super-greenhouse conditions after the first Huronian glaciation. Alternatively, if the input of reductant, such as biogenic CH_4 , to the surface system increased after the first Huronian glaciation simultaneously with an increase in O_2 production,

atmospheric O₂ levels may have been prevented from switching to a higher O₂ state after the first Huronian glaciation.

The results of this study, together with previous studies of the Huronian glaciations, suggest the possible presence of multiple (more than three) stable branches of O₂ levels in the atmosphere–ocean system, which could be contrast to the bistability model of atmospheric O₂ proposed by Goldblatt et al. (2006). At present, it is difficult to conclude whether the atmosphere–ocean system had two or more than three stable steady states of O₂ levels, given large uncertainty in the pO₂ estimated using the proxies and difference in the local depositional environments. For more quantitative estimate of pO₂, future laboratory experiments and modeling of reaction kinetics of redox-sensitive elements are required. In addition, further investigations of redox sensitive elements and MIF-S in the Espanola and Serpent formations are essential if we are to improve our understanding of the stable steady states of atmospheric O₂ levels in the early Earth system.

7. Conclusions

We measured the isotopic composition of Os, and the abundance of Os, Re, and Mo in sedimentary rocks at the boundary between the Ramsay Lake and Pecors formations, which were deposited during and immediately after the first Huronian glaciation. The enrichment of authigenic ¹⁹²Os is relatively small when normalized by Al content. However Re/Al values in the Pecors Formation are up to several times higher than the levels in average upper continental crust. Based on the results of Re–Os analysis of quartz veins in the siltstone and the Re–Os isochron diagram, we suggest that the enrichment of Os and Re were mostly hydrogenous in origin, preserving the redox conditions of the atmosphere and shallow-marine environments at the time of deposition. We found that the ¹⁸⁷Os/¹⁸⁸Os_(i) of the rock samples were close to the chondritic value, suggesting that atmospheric O₂ levels were not high enough to cause the oxidative weathering of continental Os (< 10⁻⁵–10⁻³ PAL). In contrast, the enrichment of Re may reflect the enhanced oxidative weathering of Re in the glacial aftermath under mildly oxidizing atmospheric conditions (~10⁻⁸–10⁻⁵ PAL). We also found an absence of Mo in the Pecors Formation, implying the presence of non-sulfidic conditions in shallow-marine environments at the time of deposition.

We propose that atmospheric O₂ levels would not have increased dramatically, remaining around 10⁻⁸–10⁻⁵ PAL, in the aftermath of the first Huronian glaciation, which seems to contrast with the remarkable rises in atmospheric O₂ immediately after the second and third Huronian glaciations. Based on our comparisons with geological and geochemical records, we suggest that the dramatic shifts in atmospheric O₂ after the second and third Huronian glaciations may have been caused by climatic jumps from icehouse to super-greenhouse conditions associated with the large-scale, possibly snowball, glaciations. We suggest that a step-like O₂ evolution in response to the repeated Huronian glaciations may be interpreted as transitions in the stable steady states of the O₂ level in the atmosphere–ocean system, although additional continuous records based on various proxies will be required.

Acknowledgements

The authors thank M. Ikeda, K. Ozaki, T. Nozu, M. Hailstone, A. Pace, H. Yamamoto, and Y. Otsuki for their help and advice during the study. We also thank Chris Reinhard, Simon Poulton, and one anonymous reviewer for their constructive suggestions to our earlier manuscript. This study was partly supported by Grant in Aid from Japan Society for the Promotion of Science (No. 22740352 to Y.S., No. 20109006 and 20340158 to K.S., No. 14403004 and

18340128 to E.T., No. 21840069 to T.N., and No. 21241001 and 18684032 to T.M.).

Appendix A. Supplementary material

Supplementary material related to this article can be found online at <http://dx.doi.org/10.1016/j.epsl.2013.06.018>.

References

- Anbar, A.D., Duan, Y., Lyon, T.W., Arnold, G.L., Kendall, B., Creaser, R.A., Kaufman, A.J., Gordon, G.W., Scott, C., Garvin, J., Buick, R., 2007. A whiff of oxygen before the Great Oxidation Event? *Science* 317, 1903–1906.
- Andrews, A.J., Masliwec, A., Morris, W.A., Owsiacki, L., York, D., 1986. The silver deposits at Cobalt and Gowganda, Ontario. II: An experiment in age determinations employing radiometric and paleomagnetic measurements. *Can. J. Earth Sci.* 23, 1507–1518.
- Bekker, A., Kaufman, A.J., 2007. Oxidative forcing of global climate change: A biogeochemical record across the oldest Paleoproterozoic ice age in North America. *Earth Planet. Sci. Lett.* 258, 486–499.
- Bekker, A., Holland, H.D., Wang, P.-L., Rumble III, D., Stein, H.J., Hannah, J.L., Coetzee, L.L., Buekes, N.J., 2004. Dating the rise of atmospheric oxygen. *Nature* 427, 117–120.
- Bekker, A., Kaufman, A.J., Karhu, J.A., Eriksson, K.A., 2005. Evidence for Paleoproterozoic cap carbonates in North America. *Precambrian Res.* 137, 167–206.
- Bennett, G., 2006. The Huronian Supergroup Between Sault Ste Marie and Elliot Lake. *Field Trip Guidebook*, vol. 54, Part 4. Inst. on Lake Superior Geology, Sault Ste Marie, Ontario, p. 65.
- Birck, J.L., Roy-Barman, M., Capmas, F., 1997. Re–Os isotopic measurements at the femtomole level in natural samples. *Geostand. Newsl.* 21, 19–27.
- Brookins, D.G., 1988. Eh–pH Diagrams for Geochemistry. Springer-Verlag, Berlin.
- Canfield, D.E., 2005. The early history of atmospheric oxygen: Homage to Rebert M. Garrels. *Annu. Rev. Earth Planet. Sci.* 33, 1–36.
- Claire, M.W., Catling, D.C., Zahnle, K.J., 2006. Biogeochemical modeling of the rise in atmospheric oxygen. *Geobiology* 4, 239–269.
- Cohen, A.S., Waters, F.G., 1996. Separation of osmium from geological materials by solvent extraction for analysis by thermal ionisation mass spectrometry. *Anal. Chim. Acta* 332, 269–275.
- Crusius, J., Calvert, S., Pedersen, T., Sage, D., 1996. Rhenium and molybdenum enrichments in sediments as indicators of oxic, suboxic and sulfidic conditions of deposition. *Earth Planet. Sci. Lett.* 145, 65–78.
- Dutkiewicz, A., Volk, H., George, S.C., Ridley, J., Buick, R., 2006. Biomarkers from Huronian oil-bearing fluid inclusions: An uncontaminated record of life before the Great Oxidation Event. *Geology* 34, 437–440.
- Farquhar, J., Bao, H., Thiemens, M., 2000. Atmospheric influence of Earth's earliest sulfur cycle. *Science* 289, 756–758.
- Fedo, C.M., Young, G.M., Nesbitt, H.W., Hanchar, J.M., 1997. Potassic and sodic metasomatism in the Southern Province of the Canadian Shield: Evidence from the Paleoproterozoic Serpent Formation, Huronian Supergroup, Canada. *Precambrian Res.* 84, 17–36.
- Fralick, P.W., Miall, A.D., 1989. Sedimentology of the Lower Huronian Supergroup (Early Proterozoic), Elliot Lake area, Ontario, Canada. *Sediment. Geol.* 63, 127–153.
- Goldblatt, C., Lenton, T.M., Watson, A.J., 2006. Bistability of atmospheric oxygen and the Great Oxidation. *Nature* 443, 683–686.
- Guo, Q., Strauss, H., Kaufman, A.J., Schröder, S., Gutzmer, J., Wing, B., Baker, M.A., Bekker, A., Jin, Q., Kim, S., Farquhar, J., 2009. Reconstructing Earth's surface oxidation across the Archean–Proterozoic transition. *Geology* 37, 399–402.
- Hannah, J.L., Bekker, A., Stein, H.J., Markey, R.J., Holland, H.D., 2004. Primitive Os and 2316 Ma age for marine shale: Implications for Paleoproterozoic glacial events and the rise of atmospheric oxygen. *Earth Planet. Sci. Lett.* 225, 43–52.
- Hannah, J.L., Stein, H.J., Zimmerman, A., Yang, G., Markey, R.J., Melezhik, V.A., 2006. Precise 2004 ± 9 Ma Re–Os age for Pechenga black shale: Comparison of sulfides and organic material. *Geochim. Cosmochim. Acta* 72, A228.
- Hoffman, P.F., Schrag, D.P., 2002. The snowball Earth hypothesis: Testing the limits of global change. *Terra Nova* 143, 129–155.
- Imai, N., Terashima, S., Itoh, S., Ando, A., 1995. 1994 compilation values for GSJ reference samples, "Igneous rock series". *Geochem. J.* 29, 91–95.
- Karhu, J.A., Holland, H.D., 1996. Carbon isotopes and the rise of atmospheric oxygen. *Geology* 24, 867–870.
- Kasting, J.F., 2005. Methane and climate during the Precambrian era. *Precambrian Res.* 137, 119–129.
- Kato, Y., Fujinaga, K., Suzuki, K., 2005. Major and trace element geochemistry and Os isotopic composition of metalliferous umbers from the late Cretaceous Japanese accretionary complex. *Geochem. Geophys. Geosyst.* 6, Q07004, <http://dx.doi.org/10.1029/2005GC000920>.
- Kendall, B.S., Creaser, R.A., Ross, G.M., Selby, D., 2004. Constraints on the timing of Marinoan "Snowball Earth" glaciation by ¹⁸⁷Re–¹⁸⁷Os dating of a Neoproterozoic, post-glacial black shale in Western Canada. *Earth Planet. Sci. Lett.* 222, 729–740.

- Kendall, B., Crease, R.A., Gordon, G.W., Anbar, A.D., 2009. Re–Os and Mo isotope systematics of black shales from the middle Proterozoic Velkerri and Wollgongrang Formations, McArthur Basin, northern Australia. *Geochim. Cosmochim. Acta* 73, 2534–2558.
- Kendall, B., Reinhard, C.T., Lyons, T.W., Kaufman, A.J., Poulton, S.W., Anbar, A.D., 2010. Pervasive oxygenation along late Archaean ocean margins. *Nat. Geosci.* 942, 647–652.
- Kirschvink, J.L., Gaidoes, E.J., Bertani, L.E., Beukes, N.J., Gutzmer, J., Maepa, L.N., Steinberger, R.E., 2000. Paleoproterozoic snowball Earth: Extreme climatic and geochemical global change and its biological consequences. *Proc. Natl. Acad. Sci. USA* 97, 1400–1405.
- Kopp, R.E., Kirschvink, J.L., Hilburn, I.A., Nash, C.Z., 2005. The Paleoproterozoic snowball Earth: A climate disaster triggered by the evolution of oxygenic photosynthesis. *Proc. Natl. Acad. Sci. USA* 102, 11131–11136.
- Krogh, T.E., Davis, D.W., Corfu, F., 1984. Precise U–Pb zircon and badelleyite ages for the Sudbury area. In: Pye, E.G., Naldrett, A.J., Giblin, P.E. (Eds.), *The Geology and Ore Deposits of the Sudbury Structure*. In: Ontario Geol. Surv. Spec., vol. 1, pp. 431–446.
- Levasseur, S., Birck, J.-L., Allègre, C.J., 1999. The osmium riverine flux and the oceanic mass balance of osmium. *Earth Planet. Sci. Lett.* 174, 7–23.
- Ludwig, K., 2003. *Isoplot/Ex. Version 3: A Geochronological Toolkit for Microsoft Excel*. Geochronology Center Berkeley, Berkeley.
- Maruoka, T., Koeberl, C., Hancox, P.J., Reimold, W.U., 2005. Sulfur geochemistry across a terrestrial Permian-Triassic boundary section in the Karoo Basin, South Africa. *Earth Planet. Sci. Lett.* 206, 101–117.
- McLennan, S.M., Simonetti, A., Goldstein, S.L., 2000. Nd and Pb isotopic evidence for provenance and post-depositional alteration of the Paleoproterozoic Huronian Supergroup. *Canada. Precambrian Res.* 102, 263–278.
- Melezhik, V.A., 2006. Multiple causes of Earth's earliest global glaciation. *Terra Nova* 18, 130–137.
- Morgan, J.W., Golightly, D.W., Dorrzapf, A.F., 1991. Methods for the separation of rhenium, osmium and molybdenum applicable to isotope geochemistry. *Talanta* 38, 259–265.
- Nier, A.O., 1937. The isotopic composition of osmium. *Phys. Rev.* 52, 885.
- Ogawa, N.O., Nagata, T., Kitazato, H., Ohkouchi, N., 2010. Ultra sensitive elemental analyzer/isotope ratio mass spectrometer for stable nitrogen and carbon isotopic analyses. In: Ohkouchi, N., Tayasu, I., Koba, K. (Eds.), *Earth, Life and Isotopes*. Kyoto Univ. Press, Kyoto, Japan, pp. 339–353.
- Ohkouchi, N., Nakajima, Y., Okada, H., Ogawa, N.O., Suga, H., Oguri, K., Kitazato, H., 2005. Biogeochemical processes in the saline meromictic Lake Kaiike: Implications from carbon and nitrogen isotopic compositions of photosynthetic pigments. *Environ. Microbiol.* 7, 1009–1016.
- Ono, S., Fayek, M., 2011. Decoupling of O and Pb isotope systems of uraninite in the early Proterozoic conglomerates in the Elliot Lake district. *Chem. Geol.* 288, 1–13.
- Papineau, D., Mojzsis, S.J., Schmitt, A.K., 2007. Multiple sulfur isotopes from Paleoproterozoic Huronian interglacial sediments and the rise of atmospheric oxygen. *Earth Planet. Sci. Lett.* 255, 188–212.
- Pavlov, A.A., Kasting, J.F., 2002. Mass-independent fractionation of sulfur isotopes in Archean sediments: strong evidence for an anoxic Archean atmosphere. *Astrobiology* 2, 27–41.
- Peucker-Ehrenbrink, B., Jahn, B., 2001. Rhenium-osmium isotope systematics and platinum group element concentrations: Loess and the upper continental crust. *Geochim. Geophys. Geosyst.* 2. <http://dx.doi.org/10.1029/2001GC000172>.
- Peucker-Ehrenbrink, B., Ravizza, G., 2000. The marine osmium isotope record. *Terra Nova* 12, 205–219.
- Prasad, N., Roscoe, S.M., 1996. Evidence of anoxic to oxic atmospheric change during 2.45–2.22 Ga from lower and upper sub-Huronian paleosols, Canada. *Catena* 27, 105–121.
- Ravizza, G., Turekian, K.K., 1992. The osmium isotopic composition of organic-rich marine sediments. *Earth Planet. Sci. Lett.* 110, 1–6.
- Reinhard, C.T., Raiswell, R., Scott, C., Anbar, A.D., Lyons, T.W., 2009. A late Archaean sulfidic sea stimulated by early oxidative weathering of continents. *Science* 326, 713–716.
- Robertson, J.A., 1976. The Blind River uranium deposits: The ores and their setting. *Ont. Minist. Nat. Resour. Misc. Pap.* 65, 45 pp.
- Rooney, A.D., Chew, D.M., Selby, D., 2011. Re–Os geochronology of Re–Os geochronology of the Neoproterozoic–Cambrian Dalradian Supergroup of Scotland and Ireland: Implications for Neoproterozoic stratigraphy, glaciations and Re–Os systematics. *Precambrian Res.* 185, 202–214.
- Russell, A.D., Morford, J.L., 2001. The behavior of redox-sensitive metals across a laminated-massive-laminated transition in Saanich Inlet, British Columbia. *Mar. Geol.* 174, 341–354.
- Rye, R., Holland, H.D., 1998. Paleosols and the evolution of atmospheric oxygen: A critical review. *Am. J. Sci.* 298, 621–672.
- Schidlowski, M., 2001. Carbon isotopes as biogeochemical recorders of life over 3.8 Ga of Earth history: evolution of a concept. *Precambrian Res.* 106, 117–134.
- Sekine, Y., Tajika, E., Ohkouchi, N., Ogawa, N.O., Goto, K., Tada, R., Yamamoto, S., Kirschvink, J.L., 2010. Anomalous negative excursion of carbon isotope in organic carbon after the last Paleoproterozoic glaciation in North America. *Geochim. Geophys. Geosyst.* 11, Q08019, <http://dx.doi.org/10.1029/2010GC003210>.
- Sekine, Y., Suzuki, K., Senda, R., Goto, K.T., Tajika, E., Tada, R., Goto, K., Yamamoto, S., Ohkouchi, N., Ogawa, N.O., Maruoka, T., 2011a. Osmium evidence for synchronicity between a rise in atmospheric oxygen and Palaeoproterozoic deglaciation. *Nat. Commun.* 2 (502), 1–6, <http://dx.doi.org/10.1038/ncomms1507>.
- Sekine, Y., Tajika, E., Tada, R., Hirai, T., Goto, K.T., Kuwatani, T., Goto, K., Yamamoto, S., Tachibana, S., Isozaki, Y., Kirschvink, J.L., 2011b. Manganese enrichment in the Gowganda Formation of the Huronian Supergroup: A highly oxidizing shallow-marine environment after the last Huronian glaciation. *Earth Planet. Sci. Lett.* 307, 201–210.
- Selby, D., Creaser, R.A., 2003. Re–Os geochronology of organic rich sediments: An evaluation of organic matter analysis methods. *Chem. Geol.* 200, 225–240.
- Shirey, S.B., Walker, R.J., 1995. Carius tube digestion for low-blank rhenium–osmium analysis. *Anal. Chem.* 67, 2136–2141.
- Shirey, S.B., Walker, R.J., 1998. The Re–Os isotope system in Cosmo chemistry and high-temperature geochemistry. *Annu. Rev. Earth Planet. Sci.* 26, 423–500.
- Siebert, C., Kramers, J.D., Meisel, T., Morel, P., Nägler, T.F., 2005. PGE, Re–Os, and Mo isotope systematics in Archean and early Proterozoic sedimentary systems as proxies for redox conditions of the early Earth. *Geochim. Cosmochim. Acta* 69, 1787–1801.
- Smoliar, M.I., Walker, R.J., Morgan, J.W., 1996. Re–Os ages of group IIA, IIIA, IVA, and IVB iron meteorites. *Science* 271, 1099–1102.
- Suzuki, K., Miyata, Y., Kanazawa, N., 2004. Precise Re isotope ratio measurements by negative thermal ionization mass spectrometry (NTI-MS) using total evaporation technique. *Int. J. Mass Spectrom.* 235, 97–101.
- Tejada, M.L.G., Suzuki, K., Kuroda, J., Coccioni, R., Mahoney, J.J., Ohkouchi, N., Sakamoto, T., Tatsumi, Y., 2009. Ontong Java Plateau eruption as a trigger for the early Aptian oceanic anoxic event. *Geology* 37, 855–858.
- Tribouillard, N., Algeo, T.J., Lyons, T., Riboulleau, A., 2006. Trace metals as paleoredox and paleoproductivity: An update. *Chem. Geol.* 232, 12–32.
- Turgeon, S.C., Creaser, R.A., 2008. Cretaceous oceanic anoxic event 2 triggered by a massive magmatic episode. *Nature* 454, 323–326.
- Wille, M., Kramers, J.D., Nägler, T.F., Beukes, N.J., Schröder, S., Meisel, T., Lacassie, J.P., Voegelin, A.R., 2007. Evidence for a gradual rise of oxygen between 2.6 and 2.5 Ga from Mo isotopes and Re–PGE signatures in shales. *Geochim. Cosmochim. Acta* 71, 2417–2435.
- Yamashita, Y., Takahashi, Y., Haba, H., Enomoto, S., Shimizu, H., 2007. Comparison of reductive accumulation of Re and Os in seawater-sediment systems. *Geochim. Cosmochim. Acta* 71, 3458–3475.
- Yang, G., Hannah, J.L., Zimmerman, A., Stein, H.J., Bekker, A., 2009. Re–Os depositional age for Archean carbonaceous slates from the southwestern Superior Province: Challenges and insights. *Earth Planet. Sci. Lett.* 280, 83–92.
- Young, G.M., Long, D.G.F., Fedo, C.M., Nesbitt, H.W., 2001. Paleoproterozoic Huronian basin: Product of a Wilson cycle punctuated by glaciations and a meteorite impact. *Sediment. Geol.* 141–142, 233–254.